STUDY OF PHASE TRANSFORMATIONS IN THE ROLLS OF ALLOY STEELS DURING QUENCHING BASED ON FINITE-ELEMENT MODEL

ИССЛЕДОВАНИЕ ФАЗОВЫХ ПРЕВРАЩЕНИЙ В ВАЛКАХ ИЗ ЛЕГИРОВАННЫХ СТАЛЕЙ ПРИ ЗАКАЛКЕ НА ОСНОВЕ КОНЕЧНО-ЭЛЕМЕНТНОЙ МОДЕЛИ

Dr.Sc. Bobyr S.V.[1], Dr. Krot P.V.[2], eng. Loschkarev D.V.[1], eng. Dedik M.O.[2], eng. Sharfnadel S.A.[1]
Department of structure formation and properties of ferrous metals[1] Department of Metals Forming Processes and Machines[2], – Iron and Steel Institute of Z.I. Nekrasov, National Academy of Sciences of Ukraine, Ukraine
E-mail: svbobyr07@gmail.com, paul.krot@gmail.com

Abstract/Резюме: *The studies are represented of phase and structure transformations during the process of multi-stage heat treatment of large-scale rolls. Adapted analytical models are introduced and applied to the calculation of phase transformations together with the finite-element models of rolls. The results show phase components distribution over the hardened layer of rolls of the special alloy steels 50CrMnMoV and 45Cr3MnNiMoV at different stages of the manufacturing process.*

KEYWORDS: *HEAT TREATMENT, PHASE TRANSFORMATION, FINITE-ELEMENT MODEL, ROLLS, ALLOY STEEL*

1. Introduction / Введение

Improvement of heat treatment process is efficient, if a complete picture is known of the main features and characteristics of processed alloys. Important information is about the kinetics of supercooled austenite transformation, on which the basis issues are addressed of hardenability, heat treatment schedules and the mechanical properties (YTS, UTS, E% and HB).

Experimental study of microstructure components in the heat treatment of allow steels consists of the building of time-temperature (TTT) and continuous cooling (CCT) transformation diagrams, as well as in the study of steels hardenability. At the same time, the use of numerous experimental tests to study the phase transformations are limited especially for large-scale parts. Isothermal TTT diagrams are used only for qualitative assessment of the effect of chemical composition on the process of austenite decomposition. The CCT diagrams cannot provide reliable information on the steel microstructure, if the industrial cooling schedule differs from the cooling conditions in the experiments. For this reason, CCT diagrams are only used to quantify the stability of the austenite under continuous cooling. Hardenability makes it possible to predict the structure of steel after heat treatment based on its chemical composition, which is characteristic of only a particular grade of steel. Limitations associated with the method of experimental data presentation can be eliminated by creating analytical and finite element mathematical models whose parameters are determined from the abovementioned experimental methods.

The most fundamental results in the modelling of phase transformation kinetics were obtained in works of A.N. Kolmogorov, M. Avrami, W.A. Johnson and R.F. Mehl [1-3]. The basic model known as JMAK (Johnson–Mehl–Avrami–Kolmogorov) is still widely used with various modifications where the volume of the newly formed phase is supposed dependent on the probability of nucleation centres, the linear speed of growth and the elapsed time.

Fundamental review of mathematical modelling of phase transformation process was performed by J.W. Christian [4]. In this book, it is indicated that the analytical models do not take into account the clearly non-stationary nucleation process, which is contrary to the real conditions.

Any variations of microstructure cause change of mechanical properties of the materials, therefore models were used of grains growth and refinement [5] during dynamic and static recrystallization based on C.M. Sellars equation [6] that can significantly improve metal flow patterns under plastic deformations.

Modern researches are implemented in the special purpose software packages like JMatPro or ESI Group products for steels modelling. User is able to calculate phase changes for an assigned chemical composition of steel and different modes of treatment, e.g. continuous heating and tempering. That makes it possible to predict the details of the structure after heat treatment [7-9] including large-scale rolls [10-12]. However, the possibility of universal FEM software in nonlinear thermo-mechanical models calculation with properties changing at each time step is limited to the analysis of special allow steels used for rolls manufacturing. User needs to integrate own routines for calculating diagrams of phase transformations, for example, when heat treatment is combined with cryogenic processing [13]. This opportunity can provide only advanced special purpose software products like QForm, DEFORM or MSC.Marc due to embedded interface for external user modules inclusion. Anyway, the ability to calculate a real topology of microstructure is remaining the challenge.

The aim of this work is to simulate the phase transformations during the heat treatment of large-scale rolls of special alloy steels. Simulations of multi-stage heat treatment is conducted in accordance with technological schedules of the rolls manufacturer [14], namely, stages of spray quenching and differential heat treatment (DHT). It was necessary for customer to determine the ratio of phase components in the hardened layer of rolls (50-100 mm) for various grades of new alloy steels. Additionally, the efficiency of DCT application for wear resistance of rolls is estimated by the samples of special alloy steels, 50CrMnMoV and 45Cr3MnNiMoV.

2. Theoretical models / Теоретические модели

Analytical model of austenite transformation was applied for the steel structure modelling based on the results obtained in [13, 15, 16]. The M. Avrami equation was used of the phase transformation kinetics, written in the following form:

$$P_\alpha = 1 - \exp\left(-(V\tau)^n\right), \quad (1)$$

where P_α – result of the phase transformation (amount of formed pearlite or bainite); V – relative rate of transformation; n – degree of equation; τ – time of transformation (below critical point Ac_1 for the pearlite and Ac_0 – for bainite).

The relative rate of conversion is given by [15, 16]:

$$V = K \cdot \Delta T \exp(-Q/2RT), \quad (2)$$

where $\Delta T = Tc - T$, T – current temperature; Tc – temperature critical points of transformation Ac_1 or Ac_0; Q – the activation energy of carbon diffusion in the alloy steel; K – constant coefficient; R – universal gas constant, 1.987 [cal K^{-1} mol^{-1}].

Temperature Ac_0 for roll steels is calculated from the condition that the maximum of the bainite growth rate coincides according to temperature, calculated from equation (2) and its experimental value on an isothermal diagram. This value is 500°C for steel 50CrMnMoV and 380°C for steel 45Cr3MnNiMoV.

Equation (2) describes the temperature dependence of the growth rate of transformation products in cooling steel with a maximum at certain supercooling temperature ΔT determined on the charts of isothermal transformation of austenite. This relation gives the experimental value of the diffusion activation energy Q. The steel used for model verification is 65Cr2Si3MoV with known diagrams of austenite transformation and the structure after treatment.

The exponent of the kinetic equation for the bainite transformation is given by the formula [17]:

$$n = \frac{1{,}7665}{\lg(\tau_{95\%}) - \lg(\tau_{5\%})}, \qquad (3)$$

where $\tau_{5\%}$ – the least time of 5% phase formation; $\tau_{95\%}$ – the least time of 95% phase formation. These times are determined from TTT and CCT diagrams of austenite transformation for each phase (pearlite or bainite). The maximum transformation rate was calculated using the formula:

$$V_{\max} = \sqrt[n]{0{,}0513} / \tau_{5\%} \qquad (4)$$

Based on this value V_{max}, the coefficient K is determined in formula (2). The amount of martensite formed in the steel can be calculated from the following equation:

$$P_\alpha = A_m\left(1 - \exp\left(-K_\alpha \frac{M_s - T}{T - M_f}\right)\right), \qquad (5)$$

where A_m – the amount of austenite retained to M_s temperature; M_s – temperature of the start of martensite transformation; M_f – temperature of the end of martensite transformation, K_α – coefficient of martensite formation rate at the temperature M_s.

The improved model explicitly contains the rate of phase and structure transformation (ferrite, pearlite, bainite) that allows more clearly to interpret physical coefficients. To describe the process of martensite formation, the model includes both the start and end temperature of transformation.

3. *Studies of alloy steels on models / Исследование легированных сталей на моделях*

The large-scale backup rolls for modern hot and cold rolling mills are up to 2000 mm in diameter and of 50 t weight. The main mechanical properties of rolls include the following parameters: required microstructure (tempered troostite with uniformly distributed carbides) through the whole depth of hardened layer (70-80 mm), hardness 55-65 HSD with variation 2-3 HSD, tensile strength 1200-1400 MPa. Special alloy steels 50CrMnMoV, 45Cr3MnNiMoV are used for the work rolls and backup rolls production respectively. The chemical composition of roll steels are given in Table. 1.

Table 1. *The chemical composition of rolls steels.*

Steels	Chemical composition, %						
	C	Mn	Si	Cr	Ni	Mo	V
50CrMnMoV	0.59	1.42	0.41	0.85	0.1	0.16	0.10
45Cr3MnNiMoV	0.45	0.9	0.45	2.75	0.5	0.61	0.11

Strict requirements to rolls quality are mainly satisfied due to multistage heat treatment process, which lasts up to several days. Sampling of rolls barrels for microstructure testing is almost unavailable. Therefore, mathematical model is implemented to calculate temperature and stresses. Actually, FEM modelling (Fig. 1) is practically the only way to get additional information inside the rolls for the quenching control of newly developed steels and schedules including deep cryogenic treatment for high-chromium steels. However, such models should account phase transformations to be adequate to reality that have certain issues.

Based on the changes in the yield limit of the roll material, it can be argued that the maximum voltage does not exceed 1120 MPa yield strength at the end of 2nd stage, however, are close to the value of inelastic deformation. Therefore, they should not increase the intensity of the roll cooling and reduced, but at the same time increase the quenching on the 1st or the 2nd stage.

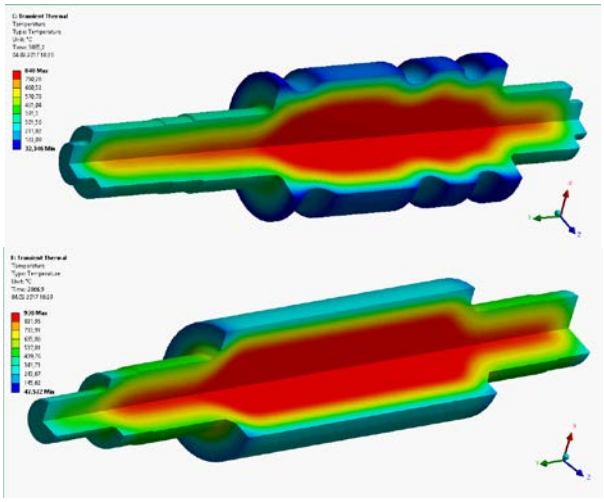

Fig. 1. *FEM models of work roll (steel 50CrMnMoV) and backup roll (steel 45Cr3MnNiMoV)*

The analytical equation of phase transformations was adopted to be applicable in the FEM modelling. The developed analytical model along with the TTT and CCT diagrams of austenite decomposition is used to analyse the structure of alloy steels 50CrMnMoV and 45Cr3MnNiMoV.

The algorithm for modeling phase transformations in rolls of alloy steels is as follows.

1) Developing the FEM model from the rolls drawings.

2) Modeling of temperature and stresses over the roll volume.

3) Calculation of critical points of phase transformations according to the regression model developed for certain range of chemical compositions of alloy steels.

4) Building of TTT for the calculated critical points.

5) Construction of a CCT by the proposed calculation method.

6) Matching the temperature curves over the roll barrel depth with the CCT diagram.

7) Calculation the boundaries of phase transformations from the cooling curves at different depths of roll and their comparison with the points of the CCT.

8) Calculation the number and fractions of microstructure components in the steel at a given depth after the end of cooling.

The analytical TTT and CCT diagrams are currently determined for a given range of chemical composition of rolls by the statistical processing of the highly alloyed steel grades. That is resulted in a possibility to take into account the complete list of alloying elements and enough wide range of their mass fraction. This is the advantage of the developed analytical models in contrast to the experimental methods of the TTT and CCT determination by the dilatometric measurements.

In steel 50CrMnMoV (Fig. 2a) there is practically no temperature range of austenite stability between the areas of perlite and bainite, which formation begins earlier than in 45Cr3MnNiMoV steel.

Under isothermal conditions, alloy steel 45Cr3MnNiMoV undergoes two transformations: pearlitic and bainitic (Fig. 2b) between which an area exists of increased stability of austenite in the temperature range 350-450°C. The region of pearlite

transformation is shifted to the right side, which indicates an increased stability of austenite due to alloying elements.

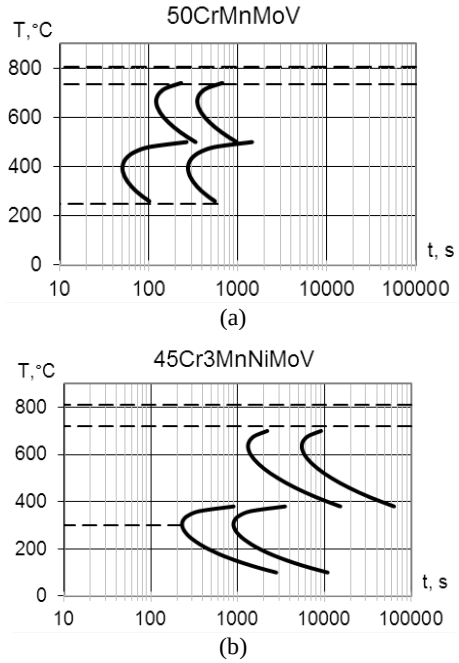

Fig. 2. *TTT diagrams of alloy steels:*
(a) 50CrMnMoV (Ac_3=810 ℃, Ac_1=757 ℃, M_s=250 ℃);
(b) 45Cr3MnNiMoV (Ac_3=815 ℃, Ac_1=720 ℃, M_s=300 ℃)

Differences in alloy elements of these steels determine the type of diagrams (Fig. 3). The steel structure 50CrMnMoV cooled at a rate 0.24°C/s (corresponds to roll depth 80 mm) has at 20°C pearlite (93%) and bainite (7 %). Steel 45Cr3MnNiMoV cooled at a rate 0.24°C/s includes at room temperature bainite (48%), martensite (47%) and retained austenite (5%).

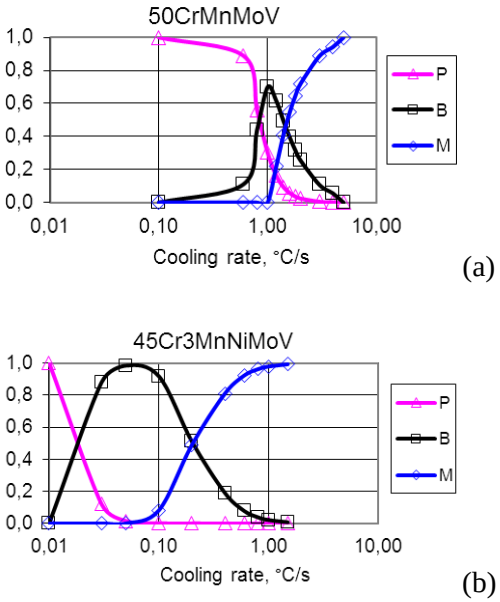

Fig. 3. *Diagrams of structure components in steels 50CrMnMoV (a) and 45Cr3MnNiMoV (b) depending on the cooling rate (P – pearlite; B – bainite; M – martensite).*

The calculated CCT of steel 50CrMnMoV has an intersection of bainite and pearlite regions at the temperature at 400°C, where these microstructure components are formed simultaneously (Fig. 3a). The areas of pearlitic and bainitic transformations for 45Cr3MnNiMoV steel (Fig. 3b) are shifted to the region of lower cooling rates compared to steel 50CrMnMoV.

Thus, the working layer of the roll at a depth of 80 mm has quenching microstructure components that provide high hardness of rolls at this depth (more than 50 HRC). The depth of rolls hardenability is assumed as the distance from the roll surface where not less than 50% of bainite and martensite are formed for this cooling rate.

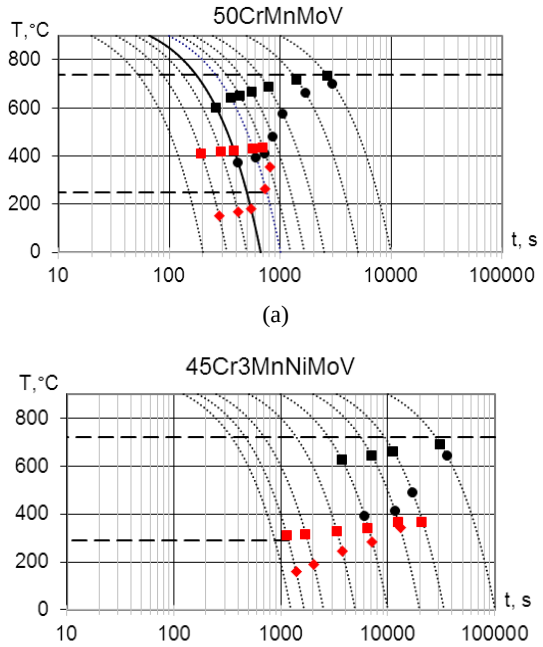

Fig. 4. *CCT diagrams of alloy steels 50CrMnMoV (a) and 45Cr3MnNiMoV (b)*

Thus, the working layer of the roll at a depth of 80 mm has quenching components of microstructure that provide high hardness of rolls at this depth (more than 50 HRC). The depth of rolls hardenability is assumed as the distance from the roll surface where not less than 50% of bainite and martensite are formed for this cooling rate.

The calculations for the 50CrMnMoV and 45Cr3MnNiMoV steels are given in Fig. 5 and 6 with roll temperatures at a depth of 0...200 mm (with increment of 20 mm). Results are obtained by the finite element model for the applicable modes of spray quenching. These graphs also contain the Ac_3, Ac_1, M_s calculated points bainite (B1, B2) transformations and regions of pearlite (P1, P2) and bainite (B1, B2) transformations from the building CCT diagrams.

3.1. Analysis of steel 50CrMnMoV

During spray quenching (I stage 0...600 s; II stage 600...1200 s) the formation of bainite is only on the surface of the roll, and perhaps to a depth of 10 mm. At a depth of 20...200 mm, the temperature is the pearlite (P1, P2) region. After termination of the cooling (2400 s) and subsequent self-heating from internal layers, roll temperature converges to an average value of about 600°C, thus bypassing the bainite region up to a depth of 120 mm and providing pearlite structure at that depth.

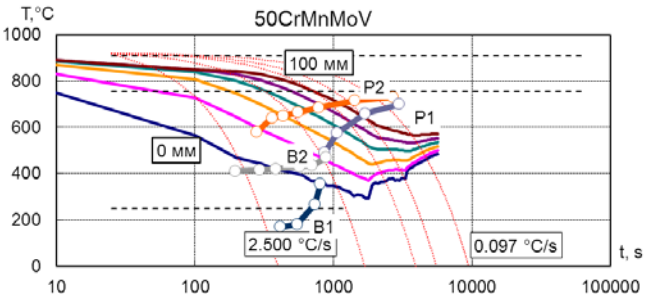

Fig. 5. *Calculations of spray quenching for work rolls of 50CrMnMoV steel*

3.2. Analysis of steel 45Cr3MnNiMoV

In the process of spray quenching (I stage 0...600 s; II stage 600...1200 s) martensite region (below Ms line) is not captured even on the roll surface. Within the whole depth of 200 mm the temperature is in the regions bainite (B1, B2) transformations. After termination of the cooling (2400 s) and subsequent self-heating from internal layers, roll temperature converges to an average value of about 600°C, slightly higher than the desired tempering temperature (500°C), thus bypassing the bainite region. Subsequent heating of the roll takes place entering the pearlite region at a depth of 20...200 mm.

The modelling of phase transformation is based on calculated CCT and TTT diagrams of 50Cr5NiMoV and 70Cr3MnNiMoV steels. Results of modelling showed their conformity by final phase composition with the experimental data. The real trajectories of cooling and rates at different points do not provide quenching structure (bainite, martensite) in the whole depth of backup rolls barrel (70 mm). For steel 50Cr5NiMoV, bainite structure is only possible in a thin surface layer (10 mm) due to self-heating from internal layers. It was recommended to increase the cooling time of the rolls at the spray-hardening machine for achieving lower temperatures at the desired depth of the roll.

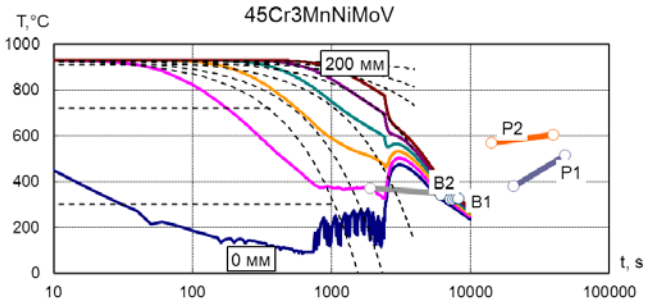

Fig. 6. *Calculations of spray quenching for backup rolls of 45Cr3MnNiMoV steel*

4. Conclusions / Заключение

The technique is improved for determining the phase composition of steels in the quenching process, allowing the calculation of the number of structural components in the steel at any time along the actual cooling trajectory at any point of the roll obtained by the finite element model.

Based on the developed regression model, isothermal and structural diagrams for 50CrMnMoV and 45Cr3MnNiMoV steels have been constructed; their correspondence to experimental data has been established. The analysis is performed of the spray quenching of rolls of alloy steels 50CrMnMoV and 45Cr3MnNiMoV, according to the existing heat treatment schedules in the rolls production.

For work roll of steel 50CrMnMoV, it is possible to obtain a bainitic structure only in a thin (up to 10 mm) near-surface layer. Corrections of schedule was proposed. While for the backup rolls of steel 45Cr3MnNiMoV, the quenching hardness and bainite with martensite microstructure is achieved through the whole depth of the working layer (up to 200 mm).

5. Literature / Литература

1. A.N. Kolmogorov, Statistical theory of crystallization of metals, Proceedings of the Academy of Sciences of the USSR, Series Math., 1937, №1 (3), 355-359.
2. M. Avrami, Kinetics of phase change, General theory, Journal of Chemical Physics, 1939, 7(12), 1103-1112.
3. W.A. Johnson, R.F. Mehl, Reaction kinetics in processes of nucleation and growth, AIME Trans., 1939,135, 416.
4. J.W. Christian, The Theory of Transformations in Metals and Alloys, 1st Ed., Pergamon Press, Oxford, UK, 2002.
5. O. Bylya, N. Biba, A. Vlasov, R. Vasin, The multidisciplinary approach to through process modelling of hot forming coupled with microstructure transformation, NAFEMS2014, Oxford, UK, June 10-11, 2014, 93-96.
6. C.M. Sellars, J.A. Whiteman, Recrystallization and Grain Growth in Hot Rolling, Metal Science, 1979, 13(3-4), 187-194.
7. B. Buchmayr, J.S. Kirkaldy, Modeling of the temperature field, transformation behavior, hardness and mechanical response of low alloy steels during cooling from the austenite region, Journal of Heat Treating, 1990, 8(2), 127-136.
8. C. Simsir, C.H. Gur, A FEM based framework for simulation of thermal treatments: Application to steel quenching, Computational Material Science, 2008, 44, 588-600.
9. A. Sugianto, M. Narazaki, M. Kogawara, A. Shirayori, Numerical simulation and experimental verification of carburising-quenching process of SCr420H steel helical gear, Journal of material processing Technology, 2009, 209(7), 3597-3609.
10. A.M. Freborg, Z. Li and B. L. Ferguson. Using Heat Treat Simulation to Characterize Sensitivity of Quench Hardening Response in Hot Mill Steel Work Rolls, Proceedings of the 23rd IFHTSE Congress, April 18–21, 2016, Savannah, Georgia, USA, pp. 428-433.
11. L. Hellenthal, C. Groth. Simulation of Residual Stresses in an Induction Hardened Roll. 23rd CADFEM Users' Meeting, International Congress on FEM Technology with ANSYS CFX & ICEM CFD Conference, November 9-11, 2005, Bonn, Germany.
12. Z.H. Liu et al. Numerical simulation of spray quenching heat-treatment process of backup roll. Advanced Materials Research, 2014, Vols. 850-851, pp 257-261.
13. P.V. Krot, S.V. Bobyr et al. Modeling of phase transformations in the rolls of the special alloy steels during quenching and deep cryogenic treatment. Proc. of 3rd Mediterranean Conf. on Heat Treatment and Surface Engineering, September 26-28, 2016, Portoroz, Slovenia, pp. 344-353.
14. V.N. Tiunov, S.A. Gritsenko, A.L. Ostapenko, et al, PAO "NKMZ" roller quenching machines, Steel in Translation, 2014, Vol. 44, Issue 12, 921-925.
15. V.I. Bolshakov, S.V. Bobyr, The kinetic parameters of pearlite formation in iron-carbon alloys, Metal Science and Heat Treatment, 2004, Vol. 8, 11-15 (in Russian).
16. V.I. Bolshakov, S.V. Bobyr, Diffusion model of transformation of austenite in carbon steels, Bulletin of Prydniprovs'ka State Academy of Civil Eng. and Arch., 2015, Vol. 7-8, 22-31 (in Russian).
17. V.M. Schastlivtsev, D.A. Mirzoev, et al, Pearlite in carbon steels, Ural Branch of Russian Academy of Sciences, Ekaterinburg, 2006 (in Russian).